

WELL-BALANCED CENTRAL-UPWIND SCHEME FOR COMPRESSIBLE TWO-PHASE FLOWS

Alexander Kurganov*

*Mathematics Department, Tulane University
6823 St. Charles Ave., New Orleans, LA 70118, USA
e-mail: kurganov@math.tulane.edu
web page: <http://www.math.tulane.edu/~kurganov/>

Key words: Godunov-Type Central-Upwind Schemes, Compressible Multi-Fluids, Well-Balanced Schemes, Nonconservative Products

Abstract. *We design a new well-balanced central-upwind scheme for compressible two-phase flows. The new scheme is an extension of the semi-discrete central-upwind scheme proposed in⁵. The novelty of the presented method is in a special discretization of non-conservative product terms, which are exactly balanced with the numerical fluxes when the method is applied to void waves. The new scheme is simpler than its predecessor and extends the applicability of central-upwind schemes to several important test problems that remained out of reach in⁵.*

1 INTRODUCTION

We consider a two-phase model that describes liquid suspensions or bubbly flows, where one is not interested in following the dynamics of individual droplets/bubbles, but rather in following the average dynamics of the fluid mixture. Following^{3,5,14}, we assume that the mixture consists of two compressible fluid components, described by their own pressure and velocity functions. The advantage of such an approach is that the resulting model is hyperbolic — a property which is lost if one fluid is assumed incompressible. To account for the fact that on the scale of interest, pressure differences between fluid components is not sustainable, infinitely fast pressure relaxation terms are included in the studied model.

In the one-dimensional case, the governing equations are:

$$\begin{pmatrix} \alpha_g \rho_g \\ \alpha_g \rho_g u_g \\ \alpha_g E_g \\ \alpha_\ell \rho_\ell \\ \alpha_\ell \rho_\ell u_\ell \\ \alpha_\ell E_\ell \end{pmatrix}_t + \begin{pmatrix} \alpha_g \rho_g u_g \\ \alpha_g (\rho_g u_g^2 + p_g) \\ \alpha_g u_g (E_g + p_g) \\ \alpha_\ell \rho_\ell u_\ell \\ \alpha_\ell (\rho_\ell u_\ell^2 + p_\ell) \\ \alpha_\ell u_\ell (E_\ell + p_\ell) \end{pmatrix}_x = \begin{pmatrix} 0 \\ P_i(\alpha_g)_x + \lambda(u_\ell - u_g) \\ U_i P_i(\alpha_g)_x + \mu P_i[p_\ell - p_g] + \lambda U_i(u_\ell - u_g) \\ 0 \\ P_i(\alpha_\ell)_x - \lambda(u_\ell - u_g) \\ U_i P_i(\alpha_\ell)_x - \mu P_i[p_\ell - p_g] - \lambda U_i(u_\ell - u_g) \end{pmatrix}, \quad (1)$$

coupled with the equation for the volume fraction:

$$(\alpha_g)_t + U_i(\alpha_g)_x = -\mu[p_\ell - p_g], \quad \alpha_g + \alpha_\ell = 1. \quad (2)$$

Here, μ is a relaxation parameter, with $\mu \rightarrow \infty$ corresponding to instantaneous relaxation, λ is a velocity relaxation parameter, α_k is the volume fraction of the k -th phase, $k \in \{\ell, g\}$, and ρ_k , u_k and E_k are its density, velocity and total energy, respectively. Near incompressibility of liquids is incorporated into the model by using a stiff equation of state (EOS):

$$E_k = \frac{1}{2}\rho_k u_k^2 + \frac{p_k + \gamma_k P_{\infty,k}}{\gamma_k - 1}, \quad (3)$$

where $P_{\infty,k}$ is a stiffness parameter, which is equal to zero for the non-stiff ideal gases. The closure equations for the interface pressure P_i and the interface velocity U_i are:

$$P_i = \alpha_g p_g + \alpha_\ell p_\ell, \quad U_i = \frac{\alpha_g \rho_g u_g + \alpha_\ell \rho_\ell u_\ell}{\alpha_g \rho_g + \alpha_\ell \rho_\ell}. \quad (4)$$

Notice that equation (2) can be combined with the first and the fourth equations in (1) and replaced with:

$$(\alpha_g \rho)_t + (\alpha_g \rho U_i)_x = -\mu \rho [p_\ell - p_g], \quad (5)$$

where $\rho = \alpha_g \rho_g + \alpha_\ell \rho_\ell$ is the total density.

While hyperbolic, the system (1),(3)–(5) is inherently nonconservative due to momentum and energy exchange terms between the phases. Computing solutions of this two-phase flow model introduces challenges due to the nonconservative form and stiffness of the governing equations and because the volume fractions (and hence, partial pressures/densities) may vanish. Several numerical methods have been recently developed for such 2-pressure 2-velocity models including the kinetic scheme³ and finite-volume upwind schemes^{1,5,14}. Godunov-type central schemes (including their recent semi-discrete central-upwind modifications^{7,8,9}) are appealing Riemann-problem-solver-free alternatives to the above methods. In⁵, a second-order central-upwind scheme has been applied to the system (1), while the transport equation (2) has been treated as a Hamilton-Jacobi equation (central-upwind schemes for Hamilton-Jacobi equations have been developed in^{2,8,10}). Such a hybrid scheme guarantees positivity of partial densities and usually does not produce negative partial pressures. The discretization of nonconservative exchange terms in⁵ was rather straightforward, and the resulting scheme worked pretty well for several sedimentation problems (in which the gas and liquid phases separate due to the gravity terms added to the studied model) and the water faucet problem from¹³. It failed, however, to produce a reliable solution in the multifluid limiting case, in which a certain region is occupied by the liquid ($\alpha_g \sim 0$), while the rest of the domain is filled with the gas ($\alpha_g \sim 1$).

In this paper, we present a new version of the semi-discrete central-upwind scheme applied to the system (1),(3)–(5), which is written in the divergence form. The non-conservative products on the right-hand side (RHS) of this system are treated as a part of the source term, whose cell average is computed using a special quadrature designed to ensure a perfect numerical balance between the nonconservative terms and the corresponding part of the fluxes. This results in a well-balanced central-upwind scheme, which resembles the well-balance central-upwind scheme for the Saint-Venant system of shallow water equations proposed in⁶.

The paper is organized as follows. In §2, we provide a brief description of the semi-discrete central-upwind schemes for hyperbolic systems of conservation and balance laws and review an operator splitting technique, required to incorporate the relaxation terms into the resulting numerical method for (1),(3)–(5). In §3, we derive a well-balanced central-upwind scheme for this system. Finally, in §4, we demonstrate the enhanced performance of the new central-upwind scheme on the examples of a void wave propagation and multifluid-fluid limits.

2 CENTRAL-UPWIND SCHEMES FOR THE TWO-PHASE SYSTEM

We first rewrite the system (1),(5) as:

$$\mathbf{w}_t + \mathbf{f}(\mathbf{w})_x = \mathbf{S}_{\text{Ex}}(\mathbf{w}) + \mathbf{S}_{\text{Rel}}(\mathbf{w}), \quad (6)$$

where the set of “conservative” variables and the corresponding fluxes are:

$$\mathbf{w} := \begin{pmatrix} \alpha_g \rho_g \\ \alpha_g \rho_g u_g \\ \alpha_g E_g \\ \alpha_\ell \rho_\ell \\ \alpha_\ell \rho_\ell u_\ell \\ \alpha_\ell E_\ell \\ \alpha_g \rho \end{pmatrix}, \quad \mathbf{F}(\mathbf{w}) := \begin{pmatrix} \alpha_g \rho_g u_g \\ \alpha_g (\rho_g u_g^2 + p_g) \\ \alpha_g u_g^2 (E_g + p_g) \\ \alpha_\ell \rho_\ell u_\ell \\ \alpha_\ell (\rho_\ell u_\ell^2 + p_\ell) \\ \alpha_\ell u_\ell^2 (E_\ell + p_\ell) \\ \alpha_g \rho U_i \end{pmatrix}, \quad (7)$$

and the nonconservative exchange terms \mathbf{S}_{Ex} and the relaxation terms \mathbf{S}_{Rel} are:

$$\mathbf{S}_{\text{Ex}} := \begin{pmatrix} 0 \\ P_i(\alpha_g)_x \\ U_i P_i(\alpha_g)_x \\ 0 \\ P_i(\alpha_\ell)_x \\ U_i P_i(\alpha_\ell)_x \\ 0 \end{pmatrix}, \quad \mathbf{S}_{\text{Rel}} := \begin{pmatrix} 0 \\ \lambda(u_\ell - u_g) \\ \mu P_i[p_\ell - p_g] + \lambda U_i(u_\ell - u_g) \\ 0 \\ -\lambda(u_\ell - u_g) \\ -\mu P_i[p_\ell - p_g] - \lambda U_i(u_\ell - u_g) \\ -\mu \rho [p_\ell - p_g] \end{pmatrix}. \quad (8)$$

Since the studied model includes (infinitely fast) relaxation terms, we apply the operator splitting technique, and at each time step the solution is evolved according to the hydrodynamic step:

$$\mathbf{w}_t + \mathbf{f}(\mathbf{w})_x = \mathbf{S}_{\text{Ex}}(\mathbf{w}), \quad (9)$$

followed by the relaxation step:

$$\mathbf{w}_t = \mathbf{S}_{\text{Rel}}(\mathbf{w}). \quad (10)$$

The ODE (10) is solved using the method described in §2.1 and §2.2 in⁵, see also¹⁴ and the hyperbolic system (9) is solved by the central-upwind scheme from⁷, which is briefly described below.

We introduce a small spatial scale Δx and, for simplicity, consider a uniform grid with $x_\beta = \beta \Delta x$. Then the cell averages of the solution,

$$\bar{\mathbf{w}}_j(t) \approx \int_{x_{j-\frac{1}{2}}}^{x_{j+\frac{1}{2}}} \mathbf{w}(x, t) dx,$$

are used to reconstruct an (essentially) non-oscillatory piecewise polynomial interpolant of an appropriate order:

$$\tilde{\mathbf{w}}(x) = \mathbf{p}_j(x), \quad x_{j-\frac{1}{2}} < x < x_{j+\frac{1}{2}}, \quad (11)$$

and to evolve the computed solution in time by solving the system of ODEs,

$$\frac{d}{dt} \bar{\mathbf{w}}_j(t) = -\frac{\mathbf{H}_{j+\frac{1}{2}}(t) - \mathbf{H}_{j-\frac{1}{2}}(t)}{\Delta x} + \frac{1}{\Delta x} \int_{x_{j-\frac{1}{2}}}^{x_{j+\frac{1}{2}}} \mathbf{S}_{\text{Ex}} dx, \quad (12)$$

where $\mathbf{H}_{j+\frac{1}{2}}$ is a numerical flux. A family of central-upwind fluxes from^{7,8} takes the following form:

$$\mathbf{H}_{j+\frac{1}{2}}(t) = \frac{a_{j+\frac{1}{2}}^+ \mathbf{f}(\mathbf{w}_{j+\frac{1}{2}}^-) - a_{j+\frac{1}{2}}^- \mathbf{f}(\mathbf{w}_{j+\frac{1}{2}}^+)}{a_{j+\frac{1}{2}}^+ - a_{j+\frac{1}{2}}^-} + a_{j+\frac{1}{2}}^+ a_{j+\frac{1}{2}}^- \left[\frac{\mathbf{w}_{j+\frac{1}{2}}^+ - \mathbf{w}_{j+\frac{1}{2}}^-}{a_{j+\frac{1}{2}}^+ - a_{j+\frac{1}{2}}^-} - \frac{\mathbf{q}_{j+\frac{1}{2}}}{2} \right]. \quad (13)$$

Here, $\mathbf{w}_{j+\frac{1}{2}}^+ := \mathbf{p}_{j+1}(x_{j+\frac{1}{2}})$ and $\mathbf{w}_{j+\frac{1}{2}}^- := \mathbf{p}_j(x_{j+\frac{1}{2}})$ are the right- and left-sided values of the piecewise polynomial reconstruction $\tilde{\mathbf{w}}$ at $x = x_{j+\frac{1}{2}}$, respectively. The one-sided local speeds of propagation, $a_{j+\frac{1}{2}}^\pm$ ($a_{j+\frac{1}{2}}^\pm$), are the positive (negative) part of the largest (smallest) eigenvalues of the Jacobian, $\frac{\partial \mathbf{f}}{\partial \mathbf{w}}$, at $x = x_{j+\frac{1}{2}}$, namely:

$$a_{j+\frac{1}{2}}^+ = \max_{k \in \{\ell, g\}, \pm} \left\{ \max \left\{ (u_k)_{j+\frac{1}{2}}^\pm + (c_k)_{j+\frac{1}{2}}^\pm, (u_k)_{j+\frac{1}{2}}^\pm - (c_k)_{j+\frac{1}{2}}^\pm, 0 \right\} \right\},$$

$$a_{j+\frac{1}{2}}^- = \min_{k \in \{\ell, g\}, \pm} \left\{ \min \left\{ (u_k)_{j+\frac{1}{2}}^\pm + (c_k)_{j+\frac{1}{2}}^\pm, (u_k)_{j+\frac{1}{2}}^\pm - (c_k)_{j+\frac{1}{2}}^\pm, 0 \right\} \right\},$$

where the first $\max_{k \in \{\ell, g, \pm\}} / \min_{k \in \{\ell, g, \pm\}}$ is taken over the corresponding “+” and “−” values of both gas and liquid components, and the speeds of sound are:

$$(c_k)_{j+\frac{1}{2}}^{\pm} = \sqrt{\frac{\gamma_k \left((p_k)_{j+\frac{1}{2}}^{\pm} + P_{\infty, k} \right)}{(\rho_k)_{j+\frac{1}{2}}^{\pm}}}, \quad k \in \{\ell, g\}.$$

Finally, $\mathbf{q}_{j+\frac{1}{2}} := \mathbf{q}(\mathbf{w}_{j+\frac{1}{2}}^{\pm}, a_{j+\frac{1}{2}}^{\pm})$ represents a “build-in” anti-diffusion term⁷, which was zero in the original central-upwind scheme in^{5,8}:

$$\mathbf{q}_{j+\frac{1}{2}} = \text{MinMod} \left(\frac{\mathbf{w}_{j+\frac{1}{2}}^+ - \mathbf{w}_{j+\frac{1}{2}}^*}{a_{j+\frac{1}{2}}^+ - a_{j+\frac{1}{2}}^-}, \frac{\mathbf{w}_{j+\frac{1}{2}}^* - \mathbf{w}_{j+\frac{1}{2}}^-}{a_{j+\frac{1}{2}}^+ - a_{j+\frac{1}{2}}^-} \right), \quad (14)$$

where

$$\mathbf{w}_{j+\frac{1}{2}}^* = \frac{a_{j+\frac{1}{2}}^+ \mathbf{w}_{j+\frac{1}{2}}^+ - a_{j+\frac{1}{2}}^- \mathbf{w}_{j+\frac{1}{2}}^- - \{ \mathbf{f}(\mathbf{w}_{j+\frac{1}{2}}^+) - \mathbf{f}(\mathbf{w}_{j+\frac{1}{2}}^-) \}}{a_{j+\frac{1}{2}}^+ - a_{j+\frac{1}{2}}^-}, \quad (15)$$

and the minmod function, given by

$$\text{MinMod}\{z_1, z_2, \dots\} := \begin{cases} \min(z_1, z_2, \dots), & \text{if } z_i > 0 \ \forall i, \\ \max(z_1, z_2, \dots), & \text{if } z_i < 0 \ \forall i, \\ 0, & \text{otherwise.} \end{cases}$$

is applied component-wise. We note that the presence of the anti-diffusion term (14)–(15) helps to minimize the amount of numerical diffusion present in the central-upwind schemes (12)–(13).

Remarks.

1. To complete the construction of the scheme (12), one needs to specify a numerical quadrature for the last term on the RHS of (12) — the cell average of the exchange terms, \mathbf{S}_{Ex} . We would like to stress that selecting this quadrature is a crucial step in designing a reliable and robust central-upwind scheme for the two-phase system.

2. The system of time-dependent ODEs (12) should be solved numerically by a stable ODE solver. In our numerical examples, we have used the third-order strong stability preserving Runge-Kutta (SSP-RK) method⁴.

3. A spatial order of the semi-discrete scheme (12)–(15) is determined by the order of the piecewise polynomial reconstruction used in (11). In our numerical experiments, we have used the second-order piecewise linear generalized minmod reconstruction (see, e.g.,^{9,11,12}):

$$\mathbf{p}_j(x) = \bar{\mathbf{w}}_j(t) + (\mathbf{w}_x)_j(x - x_j),$$

where the slopes $(\mathbf{w}_x)_j$ are computed by:

$$(\mathbf{w}_x)_j = \text{MinMod} \left\{ \theta \frac{\mathbf{w}_{j+1} - \mathbf{w}_j}{\Delta x}, \frac{\mathbf{w}_{j+1} - \mathbf{w}_{j-1}}{2\Delta x}, \theta \frac{\mathbf{w}_j - \mathbf{w}_{j-1}}{\Delta x} \right\}, \quad \theta \in [1, 2].$$

3 CONSTRUCTION OF THE WELL-BALANCED SCHEME

In this section, we derive a special quadrature for the cell average of the exchange terms, which is designed to balance them with the corresponding part of the numerical fluxes.

We consider a particular situation of a so-called void wave, that is, we assume that throughout the computational domain $u_g = u_\ell \equiv u = \text{const}$ and $p_g = p_\ell \equiv p = \text{const}$. In this case, the system (6)–(8) reduces to:

$$\mathbf{w}_t + (u\mathbf{w})_x + \begin{pmatrix} 0 \\ p\alpha_g \\ up\alpha_g \\ 0 \\ p\alpha_\ell \\ up\alpha_\ell \\ 0 \end{pmatrix}_x = \begin{pmatrix} 0 \\ p(\alpha_g)_x \\ up(\alpha_g)_x \\ 0 \\ p(\alpha_\ell)_x \\ up(\alpha_\ell)_x \\ 0 \end{pmatrix} \quad (16)$$

In fact, the last term on the left-hand side (LHS) of this equations and the term on its RHS are identical and thus, the scheme is well-balanced if the numerical discretizations of these terms coincide on void wave data as well. To guarantee this, we plug the void data into the flux difference term on the RHS of central-upwind scheme (12). For the second component ($w^{(2)} = \alpha_g \rho_g u_g$, $f^{(2)} = \alpha_g (\rho_g u_g^2 + p_g)$), we obtain:

$$\begin{aligned} H_{j+\frac{1}{2}}^{(2)}(t) &= \frac{a_{j+\frac{1}{2}}^+ f^{(2)}(\mathbf{w}_{j+\frac{1}{2}}^-) - a_{j+\frac{1}{2}}^- f^{(2)}(\mathbf{w}_{j+\frac{1}{2}}^+)}{a_{j+\frac{1}{2}}^+ - a_{j+\frac{1}{2}}^-} + a_{j+\frac{1}{2}}^+ a_{j+\frac{1}{2}}^- \left[\frac{(w^{(2)})_{j+\frac{1}{2}}^+ - (w^{(2)})_{j+\frac{1}{2}}^-}{a_{j+\frac{1}{2}}^+ - a_{j+\frac{1}{2}}^-} - \frac{q_{j+\frac{1}{2}}^{(2)}}{2} \right] \\ &= \frac{a_{j+\frac{1}{2}}^+ (\alpha_g \rho_g u_g^2)_{j+\frac{1}{2}}^- - a_{j+\frac{1}{2}}^- (\alpha_g \rho_g u_g^2)_{j+\frac{1}{2}}^+}{a_{j+\frac{1}{2}}^+ - a_{j+\frac{1}{2}}^-} + a_{j+\frac{1}{2}}^+ a_{j+\frac{1}{2}}^- \left[\frac{(w^{(2)})_{j+\frac{1}{2}}^+ - (w^{(2)})_{j+\frac{1}{2}}^-}{a_{j+\frac{1}{2}}^+ - a_{j+\frac{1}{2}}^-} - \frac{q_{j+\frac{1}{2}}^{(2)}}{2} \right] \\ &\quad + p \frac{a_{j+\frac{1}{2}}^+ (\alpha_g)_{j+\frac{1}{2}}^- - a_{j+\frac{1}{2}}^- (\alpha_g)_{j+\frac{1}{2}}^+}{a_{j+\frac{1}{2}}^+ - a_{j+\frac{1}{2}}^-} \end{aligned}$$

and hence,

$$\begin{aligned} &\frac{H_{j+\frac{1}{2}}^{(2)}(t) - H_{j-\frac{1}{2}}^{(2)}(t)}{\Delta x} \\ &= \frac{1}{\Delta x} \left\{ \frac{a_{j+\frac{1}{2}}^+ (\alpha_g \rho_g u_g^2)_{j+\frac{1}{2}}^- - a_{j+\frac{1}{2}}^- (\alpha_g \rho_g u_g^2)_{j+\frac{1}{2}}^+}{a_{j+\frac{1}{2}}^+ - a_{j+\frac{1}{2}}^-} + a_{j+\frac{1}{2}}^+ a_{j+\frac{1}{2}}^- \left[\frac{(w^{(2)})_{j+\frac{1}{2}}^+ - (w^{(2)})_{j+\frac{1}{2}}^-}{a_{j+\frac{1}{2}}^+ - a_{j+\frac{1}{2}}^-} - \frac{q_{j+\frac{1}{2}}^{(2)}}{2} \right] \right. \\ &\quad \left. - \frac{a_{j-\frac{1}{2}}^+ (\alpha_g \rho_g u_g^2)_{j-\frac{1}{2}}^- - a_{j-\frac{1}{2}}^- (\alpha_g \rho_g u_g^2)_{j-\frac{1}{2}}^+}{a_{j-\frac{1}{2}}^+ - a_{j-\frac{1}{2}}^-} - a_{j-\frac{1}{2}}^+ a_{j-\frac{1}{2}}^- \left[\frac{(w^{(2)})_{j-\frac{1}{2}}^+ - (w^{(2)})_{j-\frac{1}{2}}^-}{a_{j-\frac{1}{2}}^+ - a_{j-\frac{1}{2}}^-} - \frac{q_{j-\frac{1}{2}}^{(2)}}{2} \right] \right\} \quad (17) \end{aligned}$$

$$+ \frac{p}{\Delta x} \left\{ \frac{a_{j+\frac{1}{2}}^+(\alpha_g)_{j+\frac{1}{2}}^- - a_{j+\frac{1}{2}}^-(\alpha_g)_{j+\frac{1}{2}}^+}{a_{j+\frac{1}{2}}^+ - a_{j+\frac{1}{2}}^-} - \frac{a_{j-\frac{1}{2}}^+(\alpha_g)_{j-\frac{1}{2}}^- - a_{j-\frac{1}{2}}^-(\alpha_g)_{j-\frac{1}{2}}^+}{a_{j-\frac{1}{2}}^+ - a_{j-\frac{1}{2}}^-} \right\}.$$

We note that the first four term on the RHS of (17) represent the central-upwind approximation of the transport term $(uw^{(2)})_x$, appearing on the LHS of (16), while the last two terms approximate $p(\alpha_g)_x$ and thus, this is exactly the part of the numerical flux that should be balanced with the cell average of the corresponding exchange term. This requirement dictates the following well-balanced quadrature for the second component of the exchange term \mathbf{S}_{Ex} :

$$\frac{1}{\Delta x} \int_{x_{j-\frac{1}{2}}}^{x_{j+\frac{1}{2}}} S_{\text{Ex}}^{(2)} dx \approx \frac{P_i}{\Delta x} \left\{ \frac{a_{j+\frac{1}{2}}^+(\alpha_g)_{j+\frac{1}{2}}^- - a_{j+\frac{1}{2}}^-(\alpha_g)_{j+\frac{1}{2}}^+}{a_{j+\frac{1}{2}}^+ - a_{j+\frac{1}{2}}^-} - \frac{a_{j-\frac{1}{2}}^+(\alpha_g)_{j-\frac{1}{2}}^- - a_{j-\frac{1}{2}}^-(\alpha_g)_{j-\frac{1}{2}}^+}{a_{j-\frac{1}{2}}^+ - a_{j-\frac{1}{2}}^-} \right\}. \quad (18)$$

Similarly, we obtain the well-balanced quadratures for the third, fifth, and sixth components of \mathbf{S}_{Ex} :

$$\frac{1}{\Delta x} \int_{x_{j-\frac{1}{2}}}^{x_{j+\frac{1}{2}}} S_{\text{Ex}}^{(3)} dx \approx \frac{U_i P_i}{\Delta x} \left\{ \frac{a_{j+\frac{1}{2}}^+(\alpha_g)_{j+\frac{1}{2}}^- - a_{j+\frac{1}{2}}^-(\alpha_g)_{j+\frac{1}{2}}^+}{a_{j+\frac{1}{2}}^+ - a_{j+\frac{1}{2}}^-} - \frac{a_{j-\frac{1}{2}}^+(\alpha_g)_{j-\frac{1}{2}}^- - a_{j-\frac{1}{2}}^-(\alpha_g)_{j-\frac{1}{2}}^+}{a_{j-\frac{1}{2}}^+ - a_{j-\frac{1}{2}}^-} \right\}, \quad (19)$$

$$\frac{1}{\Delta x} \int_{x_{j-\frac{1}{2}}}^{x_{j+\frac{1}{2}}} S_{\text{Ex}}^{(5)} dx \approx \frac{P_i}{\Delta x} \left\{ \frac{a_{j+\frac{1}{2}}^+(\alpha_\ell)_{j+\frac{1}{2}}^- - a_{j+\frac{1}{2}}^-(\alpha_\ell)_{j+\frac{1}{2}}^+}{a_{j+\frac{1}{2}}^+ - a_{j+\frac{1}{2}}^-} - \frac{a_{j-\frac{1}{2}}^+(\alpha_\ell)_{j-\frac{1}{2}}^- - a_{j-\frac{1}{2}}^-(\alpha_\ell)_{j-\frac{1}{2}}^+}{a_{j-\frac{1}{2}}^+ - a_{j-\frac{1}{2}}^-} \right\}, \quad (20)$$

$$\frac{1}{\Delta x} \int_{x_{j-\frac{1}{2}}}^{x_{j+\frac{1}{2}}} S_{\text{Ex}}^{(6)} dx \approx \frac{U_i P_i}{\Delta x} \left\{ \frac{a_{j+\frac{1}{2}}^+(\alpha_\ell)_{j+\frac{1}{2}}^- - a_{j+\frac{1}{2}}^-(\alpha_\ell)_{j+\frac{1}{2}}^+}{a_{j+\frac{1}{2}}^+ - a_{j+\frac{1}{2}}^-} - \frac{a_{j-\frac{1}{2}}^+(\alpha_\ell)_{j-\frac{1}{2}}^- - a_{j-\frac{1}{2}}^-(\alpha_\ell)_{j-\frac{1}{2}}^+}{a_{j-\frac{1}{2}}^+ - a_{j-\frac{1}{2}}^-} \right\}. \quad (21)$$

This completes the derivation and the resulting well-balanced semi-discrete central-upwind scheme is (12)–(15),(18)–(21).

4 NUMERICAL EXAMPLES

We now demonstrate the performance of the well-balanced central-upwind scheme on three numerical examples taken from⁵. In Example 1, we compare the results obtained by the new and original versions of the central-upwind schemes. Examples 2 and 3 are only solved by the new central-upwind scheme since the scheme from⁵ is not applicable in the limiting multifluid case.

Example 1 — Void Wave Propagation

In this example, we consider the initial data that corresponds to a void wave:

$$\begin{cases} (\rho_g, \rho_\ell, \alpha_g) = (2, 1, 0.1), & x < 0.5, \\ (\rho_g, \rho_\ell, \alpha_g) = (1, 2, 0.9), & x > 0.5, \end{cases} \quad (22)$$

$$u_g = u_\ell = p_g = p_\ell = 1, \quad \gamma_g = 1.4, \quad \gamma_\ell = 1.2, \quad P_{\infty,g} = P_{\infty,\ell} = 0.$$

The initial-value problem (IVP) (6)–(8),(22) is solved by both the new well-balanced central-upwind scheme (12)–(15),(18)–(21) and its original version from⁵. The obtained solutions are shown in Figure 1. Both solutions are computed at time $t = 0.1$ using the same uniform grid with $\Delta x = 1/200$. One can clearly see that unlike the original central-upwind scheme, the new one preserves the mechanical equilibrium between the phases, that is, both ρ , U_i and P_i remain constant.

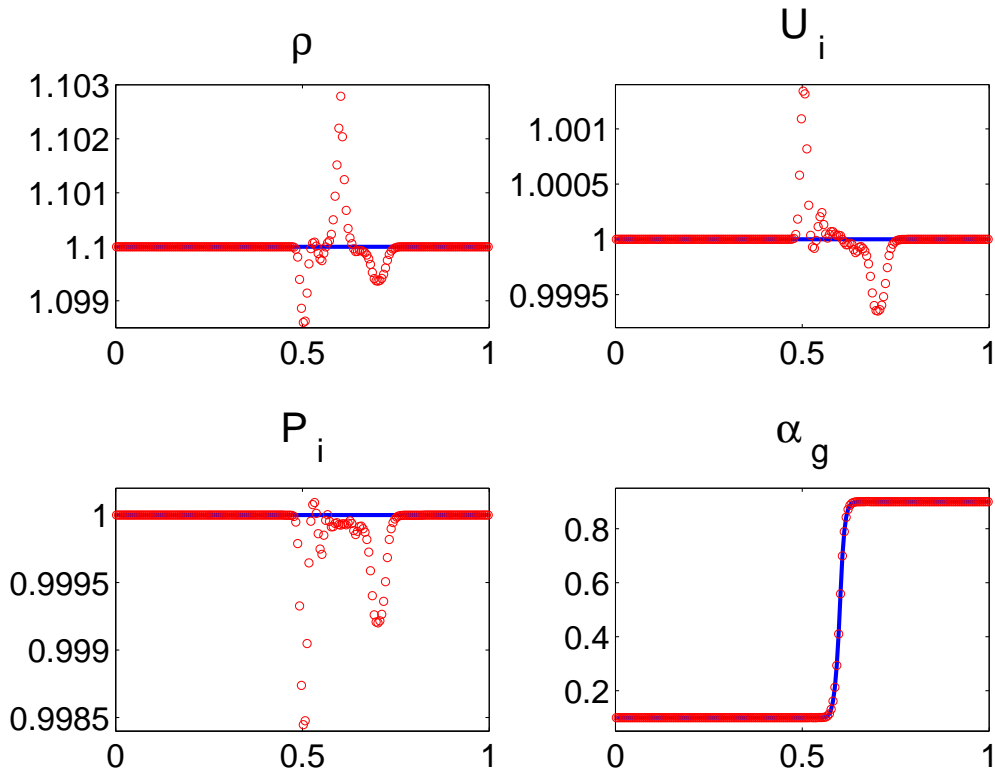


Figure 1: IVP (6)–(8),(22) by the well-balanced (solid line) and original (circles) central-upwind schemes.

Example 2 — Air-Helium Multifluid Limit

Next, we consider a multifluid limiting case when the air and helium are initially separated by a sharp interface and the mixing is avoided by including both pressure and velocity instantaneous relaxation rates ($\lambda = \mu = \infty$). The initial data are:

$$\begin{cases} \alpha_g = 10^{-8} \sim 0, & x < 0.5, \\ \alpha_g = 1 - 10^{-8} \sim 1, & x > 0.5, \end{cases} \quad (23)$$

$$(\rho_g, u_g, p_g, \gamma_g, P_{\infty,g}) = (4/29, 0, 0.1, 5/3, 0),$$

$$(\rho_\ell, u_\ell, p_\ell, \gamma_\ell, P_{\infty,\ell}) = (1, 0, 1, 1.4, 0).$$

The solutions, computed by the well-balanced central-upwind scheme (12)–(15),(18)–(21) on both coarse ($\Delta x = 1/400$) and fine ($\Delta x = 1/5000$) grids are shown in Figure 2. The final computational time is $t = 0.2$. One can observe a superior resolution achieved by the new scheme and lack of any interface pressure/velocity oscillations.

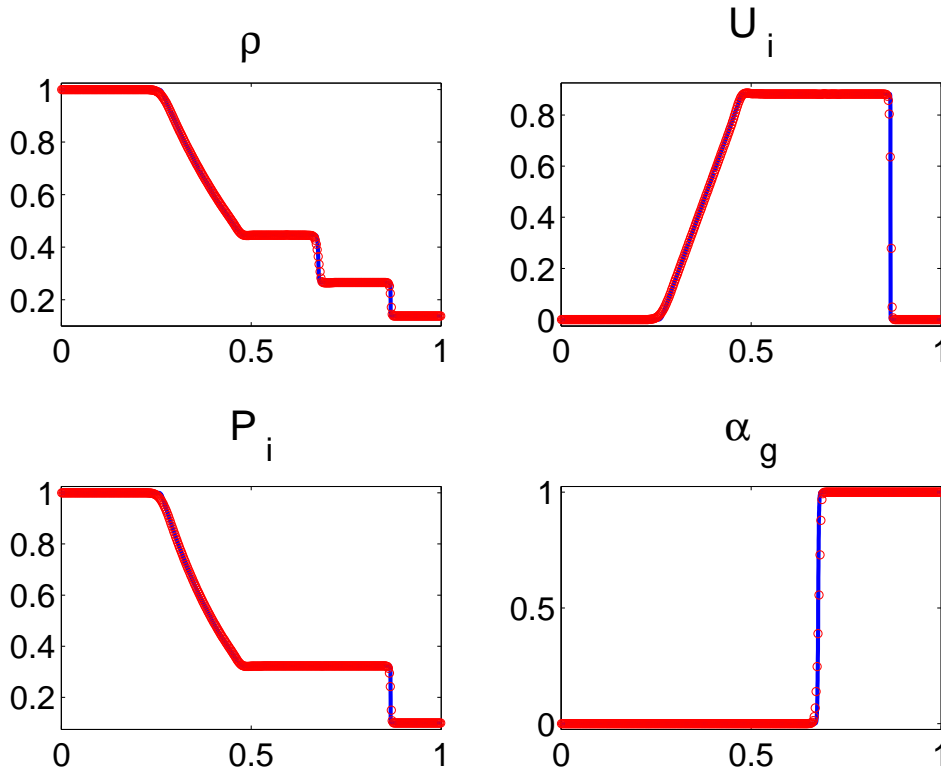


Figure 2: IVP (6)–(8),(23) by the well-balanced central-upwind scheme with $\Delta x = 1/400$ (circles) and $\Delta x = 1/5000$ (solid line).

We note that even though our scheme does not guarantee positivity of computed partial pressures, $\alpha_g p_g$ and $\alpha_\ell p_\ell$, they remained positive even when smaller (than 10^{-8}) values of α_g and α_ℓ were used.

Example 3 — Water-Air Multifluid Limit

Finally, we consider another multifluid limiting case, in which the water (modeled by the stiff equation of state) and air are initially separated by a sharp interface. As in the previous example, the relaxation parameters are infinite so that no fluid mixing is allowed. We solve the system (6)–(8) subject to the following initial data:

$$\begin{cases} \alpha_g = 10^{-8} \sim 0, & x < 0.75, \\ \alpha_g = 1 - 10^{-8} \sim 1, & x > 0.75, \end{cases} \quad (24)$$

$$(\rho_g, u_g, p_g, \gamma_g, P_{\infty,g}) = (65, 0, 10^5, 1.4, 0),$$

$$(\rho_\ell, u_\ell, p_\ell, \gamma_\ell, P_{\infty,\ell}) = (1000, 0, 10^9, 4.4, 6 \cdot 10^8).$$

The solutions at time $t = 0.00025$ computed by the well-balanced central-upwind scheme (12)–(15),(18)–(21) on two different uniform grids are shown in Figure 3. Once again, the quality of the obtained solutions is high and no pressure/velocity oscillations have been generated near the material interface. Also notice a very good resolution of the “narrow” intermediate state, demonstrated in Figure 4.

Acknowledgment

This work was supported in part by the NSF Grant # DMS-0310585. The author would like to thank Professor S. Karni from the University of Michigan for a number of stimulating discussions. A significant part of this work was done in Fall 2005, when the author visited the Department of Mathematics of the University of Michigan. The author would like to thank the chairman Professor A. Bloch and all members of the department for their extremely warm hospitality.

REFERENCES

- [1] R. Abgrall and R. Saurel. Discrete equations for physical and numerical compressible multiphase flow mixtures. *J. Comput. Phys.*, **186**, 361–396, (2003).
- [2] S. Bryson, A. Kurganov, D. Levy and G. Petrova. Semi-discrete central-upwind schemes with reduced dissipation for Hamilton-Jacobi equations. *IMA J. Numer. Anal.*, **25**, 113–138, (2005).
- [3] F. Coquel, K. El Amine, E. Godlewski, B. Perthame and P. Rascle. A numerical method using upwind schemes for the resolution of two-phase flows. *J. Comput. Phys.*, **136**, 272–288, (1997).
- [4] S. Gottlieb, C.-W. Shu and E. Tadmor. High order time discretization methods with the strong stability property. *SIAM Rev.*, **43**, 89–112, (2001).
- [5] S. Karni, E. Kirr, A. Kurganov and G. Petrova. Compressible two-phase flows by central and upwind schemes. *M2AN Math. Model. Numer. Anal.*, **38**, 477–493, (2004).

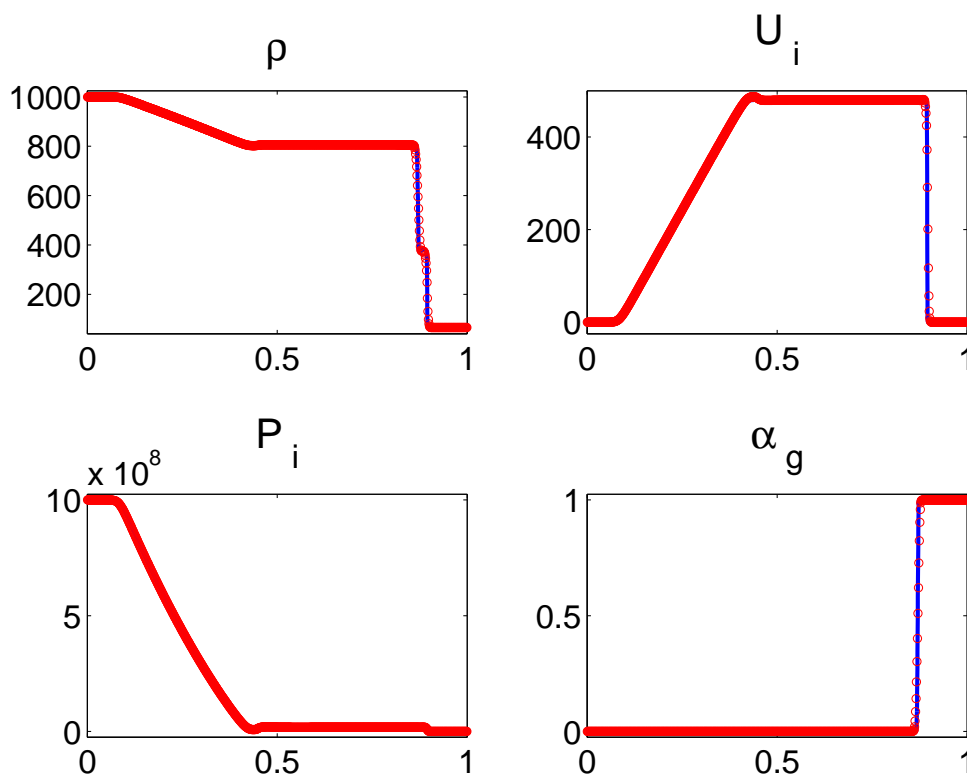


Figure 3: IVP (6)–(8),(24) by the well-balanced central-upwind scheme with $\Delta x = 1/800$ (circles) and $\Delta x = 1/3200$ (solid line).

- [6] A. Kurganov and D. Levy. Central-upwind schemes for the Saint-Venant system. *M2AN Math. Model. Numer. Anal.*, **36**, 397–425, (2002).
- [7] A. Kurganov and C.-T. Lin. On the reduction of numerical dissipation in central-upwind schemes. Submitted to *Commun. Comput. Phys.*
- [8] A. Kurganov, S. Noelle and G. Petrova. Semi-discrete central-upwind scheme for hyperbolic conservation laws and Hamilton-Jacobi equations. *SIAM J. Sci. Comput.*, **23**, 707–740, (2001).
- [9] A. Kurganov and E. Tadmor. New high-resolution central schemes for nonlinear conservation laws and convection-diffusion equations. *J. Comput. Phys.*, **160**, 241–282, (2000).
- [10] A. Kurganov and E. Tadmor. New high-resolution semi-discrete schemes for Hamilton-Jacobi equations. *J. Comput. Phys.*, **160**, 720–742, (2000).

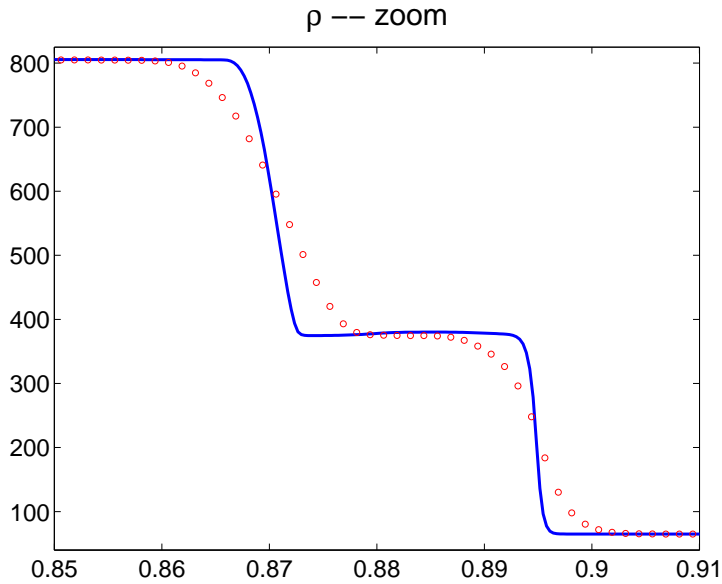


Figure 4: Density (zoom) by the well-balanced central-upwind scheme with $\Delta x = 1/800$ (circles) and $\Delta x = 1/3200$ (solid line).

- [11] B. van Leer. Towards the ultimate conservative difference scheme, V. A second order sequel to Godunov's method. *J. Comput. Phys.*, **32**, 101–136, (1979).
- [12] H. Nessyahu and E. Tadmor. Non-oscillatory central differencing for hyperbolic conservation laws. *J. Comput. Phys.*, **87**, 408–463, (1990).
- [13] V.H. Ransom. *Numerical benchmark tests*, G.F. Hewitt, J.M. Delhay and N. Zuber Eds., Hemisphere, Washington, DC, Multiphase Science and Technology, Vol. 3, (1987).
- [14] R. Saurel and R. Abgrall. A multiphase Godunov method for compressible multifluid and multiphase flows. *J. Comput. Phys.*, **150**, 425–467, (1999).